Spectroscopic factors and level spectra in neutron-rich Sn isotopes

H. K. Wang [1,2,*], Y. J. Li [3], Y. B. Wang [3], A. Jalili [1], and Y. B. Qian [4,†]

[1]*Department of Physics, Zhejiang SCI-TECH University, Hangzhou 310018, China*

[2]*School of Physics and Astronomy, Shanghai Jiao Tong University, Shanghai 200240, China*

[3]*China Institute of Atomic Energy, P.O. Box 275(10), Beijing 102413, China*

[4]*Department of Applied Physics and MIIT Key Laboratory of Semiconductor Microstructure and Quantum Sensing, Nanjing University of Science and Technology, Nanjing 210094, China*

The Hamiltonian including core excitations and the intruder orbit $i_{13/2}$ is used to investigate spectroscopic factors and level spectra in neutron-rich Sn isotopes. The state $13/2^+$ of ^{131}Sn is predicted with a relative small value of spectroscopic factor, since the competition driven by pair cross-shell excitations weakens the single particle properties of this high-lying state near 5 MeV. The level $11/2^-$ of ^{133}Sn is predicted at 3.6 MeV coupled by cross-shell configuration $\nu h_{11/2}^{-1} f_{7/2}^2$. In ^{135}Sn, the state $3/2^+$ is predicted at 2.66 MeV with a main cross-shell configuration $\nu d_{3/2}^{-1} f_{7/2}^4$, and the state $13/2^+$ at about 2.5 MeV is predicted as a good isomer coupled by intruder orbit $i_{13/2}$. The level 3^- of ^{134}Sn(^{136}Sn) is predicted as a good isomer, due to the γ decay blocked by the spin-trap structures. The level $13/2^+$ of ^{137}Sn is predicted at about 2.1 MeV with 49% of configuration $\nu f_{7/2}^4 i_{13/2}$. The ground state of ^{137}Sn is predicted as $7/2^-$ level with a main configuration $\nu f_{7/2}^5$. This work emphasizes the importance of the intruder orbit $i_{13/2}$ to explain level spectra of neutron-rich Sn isotopes, and these predictions would provide useful guidance for further experiments in this nuclei region.

I. INTRODUCTION

The shell model theory describes well the magic numbers of protons and/or neutrons such as 2, 8, 28, 50, and 82, as well as 126 for neutrons [1]. The nuclei with these magic numbers have comparatively high energies of the first excited 2^+ state, as well as high energies needed to remove their nucleon(s) [2]. It is essential to investigate single-particle states outside a double-shell closure in order to modify theoretical models and predict the properties of unmeasured nuclei [3–9]. The rapid neutron-capture process (r process) is suggested producing more than half of the nuclei heavier than iron [10]. The structural inputs of unmeasured nuclei are from predictions of nuclear models [11]. Therefore, it is necessary to develop a suitable interaction for these unstable nuclei.

The spectroscopic factors can be used to calculate direct-semidirect (n, γ) cross sections that are important inputs for r-process abundance calculations [12]. The spectroscopic factors are critical test for the single-particle states outside the closed shell with magic number. If nucleus A has a good magic number, high spectroscopic factors mean the single-particle strength in a specific orbital of the $A + 1$ nucleus is concentrated in one state. The experimental energies of single-particle states just outside a shell closure are necessary benchmarks for shell-model calculations of neutron-rich nuclei [13–16]. The single-particle properties of ^{133}Sn have

been experimentally confirmed by β-decay measurements and the spectroscopy of prompt γ rays after the fission of ^{248}Cf [17,18].

The transfer reaction is a highly sensitive technique for studying single-particle states, in which a single nucleon is transferred from one nucleus to another [19]. By performing the ^{132}Sn(d, p) ^{133}Sn reaction in inverse kinematics, the purity of low-spin single-neutron excitations have been determined experimentally in ^{133}Sn [2]. In theory, both low-lying states and high cross-shell excitations have been described well in the neutron-rich nuclei near ^{132}Sn [20–22]. Recently, a regular correlation driven by the monopole interaction was found between the neutron orbits $h_{11/2}$ and $d_{3/2}$ in the hole nuclei region of ^{132}Sn. The ground-state inversions from ^{130}In (^{129}Cd) to ^{128}In (^{127}Cd) observed experimentally were explained well for the first time by this correlation [23].

In ^{131}Sn, the spectroscopic factors of high-lying single particle states have been observed by the ^{130}Sn(d, p) ^{131}Sn reaction [24]. The low-lying single particle states of ^{131}Sn, namely, $3/2^+$, $11/2^-$, $1/2^+$, $5/2^+$, and $7/2^+$ under $N = 82$ shell, have been successfully reproduced in the hole-nuclei model space [15]. However, these high-lying single particle states of ^{131}Sn above the $N = 82$ shell cannot be well investigated, due to the absence of single particle orbits above $N = 82$ in this model space. Recently, a new Hamiltonian has been established by including both cross-shell excitations and neutron intruder orbit $i_{13/2}$ [25]. In this new Hamiltonian, the major shell $N = (82, 126)$ with additional two orbits under $N = 82$ is suitable to describe the observed single particle states in hole nucleus ^{131}Sn.

*whk2007@163.com
†qyibin@njust.edu.cn

In this paper, we will investigate the spectroscopic factors and low-lying states of neutron-rich Sn isotopes by using the Hamiltonian in Ref. [25]. The shell-model codes NUSHELLX@MSU and KSHELL are used for calculations [26,27].

II. HAMILTONIAN AND MODEL SPACE

We use the Hamiltonian of extended paring plus multipole forces with monopole correction terms (EPQQM) in the proton-neutron representation:

$$
\begin{aligned}
H &= H_{\text{sp}} + H_{P_0} + H_{P_2} + H_{QQ} + H_{OO} + H_{HH} + H_{\text{mc}} \\
&= \sum_{\alpha,i} \varepsilon_a^i c_{\alpha,i}^\dagger c_{\alpha,i} - \frac{1}{2} \sum_{J=0,2} \sum_{ii'} g_{J,ii'} \sum_M P_{JM,ii'}^\dagger P_{JM,ii'} \\
&\quad - \frac{1}{2} \sum_{ii'} \frac{\chi_{2,ii'}}{b^4} \sum_M : Q_{2M,ii'}^\dagger Q_{2M,ii'} : \\
&\quad - \frac{1}{2} \sum_{ii'} \frac{\chi_{3,ii'}}{b^6} \sum_M : O_{3M,ii'}^\dagger O_{3M,ii'} : \\
&\quad - \frac{1}{2} \sum_{ii'} \frac{\chi_{4,ii'}}{b^8} \sum_M : H_{4M,ii'}^\dagger H_{4M,ii'} : \\
&\quad + \sum_{a\leqslant c,ii'} k_{\text{mc}}(ia, i'c) \sum_{JM} A_{JM}^\dagger(ia, i'c) A_{JM}(ia, i'c).
\end{aligned}
\tag{1}
$$

This equation has the single-particle Hamiltonian (H_{sp}), the $J=0$ and $J=2$ pairing ($P_0^\dagger P_0$ and $P_2^\dagger P_2$), the quadrupole-quadrupole ($Q^\dagger Q$), the octupole-octupole ($O^\dagger O$), the hexadecapole-hexadecapole ($H^\dagger H$) terms, and the monopole corrections (H_{mc}). $P_{JM,ii'}^\dagger$ and $A_{JM}^\dagger(ia, i'c)$ are the pair operators in the pn representation. $Q_{2M,ii'}^\dagger$, $O_{3M,ii'}^\dagger$, and $H_{4M,ii'}^\dagger$ are the quadrupole, octupole, and hexadecapole operators, respectively, and the i (i') are the indices of protons (neutrons). The parameters of $g_{J,ii'}$, $\chi_{2,ii'}$, $\chi_{3,ii'}$, $\chi_{4,ii'}$, and $k_{\text{mc}}(ia, i'c)$ are the force strengths, and b is the harmonic-oscillator range parameter.

The model space of this Hamiltonian selected five proton orbits above $Z = 50$ ($0g_{7/2}, 1d_{5/2}, 1d_{3/2}, 2s_{1/2}, 0h_{11/2}$), and six neutron orbits above $N = 82$ ($1f_{7/2}, 2p_{3/2}, 2p_{1/2}, 0h_{9/2}, 1f_{5/2}, 0i_{13/2}$). Furthermore, the proton orbit of $0g_{9/2}$ under $Z = 50$ and neutron orbit of $1d_{3/2}$ and $0h_{11/2}$ under $N = 82$ were included for cross-shell excitations. In ^{131}Sn, three neutrons are allowed to cross the $N = 82$ shell, one from orbit $1d_{3/2}$ and two from orbit $0h_{11/2}$.

We keep the same parameters of two-body strengths, and five monopole terms are employed as reported in Ref. [25]:

$$
\begin{aligned}
Mc1 &\equiv k_{\text{mc}}(\nu h_{11/2}, \nu f_{7/2}) = 0.35 \,\text{MeV}, \\
Mc2 &\equiv k_{\text{mc}}(\nu d_{3/2}, \nu f_{7/2}) = 0.45 \,\text{MeV}, \\
Mc3 &\equiv k_{\text{mc}}(\pi g_{7/2}, \nu h_{9/2}) = -1.6 \,\text{MeV}, \\
Mc4 &\equiv k_{\text{mc}}(\pi g_{7/2}, \nu i_{13/2}) = -0.8 \,\text{MeV}, \\
Mc5 &\equiv k_{\text{mc}}(\pi h_{11/2}, \nu f_{7/2}) = -1.5 \,\text{MeV}.
\end{aligned}
\tag{2}
$$

The force strength of these five monopole terms have been determined by the data of nuclei ^{133}Sb, ^{134}Sb, ^{134}Te, ^{135}Te, and ^{135}I. Due to missing three-body contributions, the monopole corrections are necessary for shell-model calculations with two-body interactions [28,29].

III. SPECTROSCOPIC FACTORS

Spectroscopic factors provide the cross-section information of nuclear single-particle configurations, which are crucial in one-nucleon transfer reactions [30,31]. The cross section of transfer reactions, in which one particle is removed, is proportional to the summing of matrix elements over m, final M states (M_j), and initial M states (M_i):

$$
\begin{aligned}
\sigma^- &\sim \sum_{m,M_{f,i}} \frac{\left|\langle \psi_f^{A-1} J_f M_f | \tilde{a}_{k,m} | \psi_i^A J_i M_i \rangle\right|^2}{2J_i + 1} \\
&= \frac{1}{2J_i + 1} \left|\langle \psi_f^{A-1} J_f || \tilde{a}_k || \psi_i^A J_i \rangle\right|^2.
\end{aligned}
\tag{3}
$$

The a_k^+ is the creation operator that creates the single-particle state $|k\rangle$. The $\tilde{a}_k$ is the conjugate of destruction operator a_k.

If one describes the final lighter nucleus by the wave function $|\psi_f^{A-1} J_f\rangle$, and the initial heavier nucleus by $|\psi^A J_i\rangle$, the spectroscopic factor can be defined as

$$
\begin{aligned}
S &= \frac{1}{2J_i + 1} \left|\langle \psi_f^{A-1} J_f || \tilde{a}_k || \psi_i^A J_i \rangle\right|^2 \\
&= \frac{1}{2J_i + 1} \left|\langle \psi_i^A J_i || a_k^+ || \psi_f^{A-1} J_f \rangle\right|^2 \\
&\sim \sigma^-.
\end{aligned}
\tag{4}
$$

If the removal of one particle in orbit k is calculated as the cross section of a single particle (σ_{sp}), one has

$$
\sigma^- = S\sigma_{\text{sp}}.
\tag{5}
$$

Similarly obtain the cross section of reactions adding one particle (σ^+),

$$
\begin{aligned}
\sigma^+ &\sim \frac{1}{2J_i + 1} \left|\langle \psi_f^{A+1} J_f || a_k^+ || \psi_i^A J_i \rangle\right|^2 \\
&= \frac{2J_f + 1}{2J_i + 1} S,
\end{aligned}
\tag{6}
$$

where S means the spectroscopic factor removing a particle from $A + 1$ to A, and we also have

$$
\sigma^+ = \frac{2J_f + 1}{2J_i + 1} S\sigma_{\text{sp}}.
\tag{7}
$$

If the final state is formed by coupling the odd nucleon j and the closed core without any fragmentation, one can obtain a spectroscopic factor of 1, since the overlap integral is unity.

IV. SINGLE-PARTICLE STATES

Due to the additional cross-shell orbits $0h_{11/2}$ and $1d_{3/2}$ in the model space above $N = 82$ [25], we can investigate the observed high-lying states of hole nucleus ^{131}Sn, namely $7/2^-$, $3/2^-$, $1/2^-$, and $5/2^-$ states. These states have good
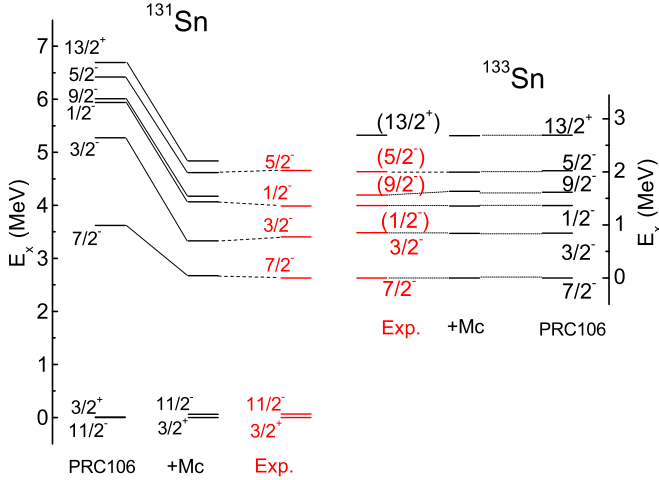
FIG. 1. Single-particle-state centroids above $N = 82$ obtained from the diagonalization. Results of column PRC106 calculated by the interaction in Ref. [25]. The column +Mc of ^{131}Sn means adding monopole corrections (see text). Corresponding data (Exp.) are from [2].

TABLE I. The spectroscopic factors of single-particle-state centroids obtained from the diagonalization. Corresponding data are from Ref. [2].

J^π	E_x	MeV		S		
^{133}Sn	Exp.	Th.1	Th.2	Exp.	Th.1	Th.2
$(7/2^-)$	0	0	0	0.86	0.98	0.95
$(3/2^-)$	0.854	0.846	0.840	0.92	0.97	0.94
$(1/2^-)$	1.363	1.367	1.358	1.1	0.97	0.94
$(9/2^-)$	1.561	1.618	1.635	0.99	0.97	
$(5/2^-)$	2.005	2.023	1.994	1.1	0.97	0.89
$(13/2^+)$		2.693	2.682	0.97		0.94
^{131}Sn	Exp.	Th.1	Th.2	Exp.	Th.1	Th.2
$(7/2^-)$	2.628	3.62	2.674	0.7	0.90	0.88
$(3/2^-)$	3.404	5.273	3.332	0.7	0.97	0.41
$(1/2^-)$	3.986	5.941	4.067	1	0.71	0.54
$(9/2^-)$		6.01	4.174		0.58	0.43
$(5/2^-)$	4.655	6.421	4.616	0.75	0.35	0.35
$(13/2^+)$		6.693	4.836		0.29	0.20

single particle properties, according to their big values of spectroscopic factors from experiment. As shown in Fig. 1, these high-lying states of ^{131}Sn around 4 MeV are similar to single particle states in ^{133}Sn. The column marked "PRC106" is calculations of ^{131}Sn by the Hamiltonian in Ref. [25] with the same two-body strengths and monopole correction terms.

The states in column PRC106 are somewhat high, since this Hamiltonian is designed for particle nuclei above the $N = 82$ shell. Therefore, monopole correction terms between the orbit $\nu h_{11/2}$ and the major shell of $N = (82, 126)$ (marked with +Mc in Fig. 1) are considered to account for the truncation effects of the model space. With average strength 1.0 MeV, these additional monopole terms are only considered to the hole-nucleus ^{131}Sn under the $N = 82$ shell. They reproduce the high-lying single-particle-state centroids in ^{131}Sn well, and have almost no effects on the low-lying levels of ^{133}Sn. We test such monopole corrections by comparing with datum 2^+ at 4.041 MeV in ^{132}Sn. Its theoretical value reduces to 4.099 MeV from 4.649 MeV. The difference factor is 1.01 (1.15 before). These corrections between neutron orbit $0h_{11/2}$ and the major shell of $N = (82, 126)$ are beneficial to deal with hole nucleus ^{131}Sn closing to the $N = 82$ shell.

Single-particle states outside a double-shell closure are necessary for calibrating theoretical interactions and predicting properties of unknown nuclei. The single-particle states in ^{133}Sn were measured by the inverse kinematics technique transferring a single nucleon to the nucleus [2]. In ^{133}Sn, the single neutron orbits $2f_{7/2}, 3p_{3/2}, 1h_{9/2}, 3p_{1/2}, 2f_{5/2}$ have been confirmed in the (d, p) reaction on the doubly magic ^{132}Sn [2], while the value of the neutron $\nu 1i_{13/2}$ is only suggested by Ref. [18]. These states lie outside the double shell closure of the short-lived nucleus ^{132}Sn, and their purity can clearly illustrate the magic nature of ^{132}Sn.

For spectroscopic factors in ^{133}Sn, this work reproduce well $(7/2^-)$, $(3/2^-)$, $(1/2^-)$, and $(5/2^-)$. The predicted spectroscopic factor of state $9/2^-$ is 0.97, of state $(13/2^+)$ is 0.94

(Table I). Similar single particle states of $l = 1, 3$ are also observed in low-lying spectra of ^{131}Sn through the inverse ^{130}Sn (d, p) ^{131}Sn reaction at 4.8 MeV/u. The observations of $(1/2^-)$ and $(3/2^-)$ states with $l = 1$ are important for direct neutron capture that is crucial for r-process nucleosynthesis. The two $l = 1$ single particle states are reported bound, which mean a relatively large cross section of direct neutron capture [24]. The concentrative single-particle states of $l = 1, 3$ confirm the stableness of the proton $Z = 50$ core, and a simple neutron structure outside the core ^{130}Sn.

By comparing with single particle states of ^{133}Sn, the lack of states $9/2^-$ and $13/2^+$ in experiment is due to the rather weakness of $l = 5, 6$ transfers in the ^{130}Sn (d, p) ^{131}Sn reaction. As shown in Table I, the lowest $13/2^+$ state, predicted at 4.8 MeV, has a spectroscopic factor 0.20, which is small, but at the same time is the largest among the $i_{13/2}$ spectroscopic factors of the other $13/2^+$ states. The sum of the $i_{13/2}$ spectroscopic factors over all calculated $13/2^+$ states is about 0.9424, which almost exhausts the sum rule.

Note the state $13/2^+$ at 4.8 MeV only has 21% of configuration $\nu h_{11/2}^{-2} i_{13/2}$ (A), while 59% is a configuration of $\nu h_{11/2}^{-2} d_{3/2}^{-1} f_{7/2}^2$ (B). The configuration (A) contributes to the single particle properties by one neutron occupying the single particle orbit $i_{13/2}$. The configuration (B) represents pair cross-shell excitations as two neutrons are excited across the $N = 82$ shell and occupy the orbit $f_{7/2}$. The neutron-pair excitation occurs from $h11/2$ to $f7/2$ orbits and thus cross the $N = 82$ shell gap. The competition driven by double cross-shell excitations weakens the single particle properties of the high-lying state $13/2^+$ in ^{131}Sn.

The low-lying states and spectroscopic factors of ^{133,135,137}Sn are calculated under the same model-space truncation without cross-shell excitations (Fig. 2). Considering greater valence neutrons in ^{137}Sn, orbits under $N = 82$ have to freeze out for keeping the truncation consistently in these three nuclei. In this truncation, the dimension of ^{137}Sn is less than 10^5. If considering one cross-shell neutron excited
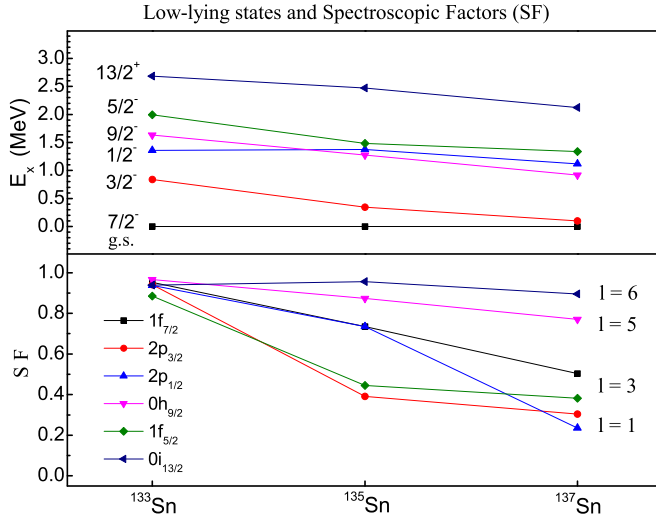
FIG. 2. Low-lying states and spectroscopic factors in nuclei ^{133,135,137}Sn.

from orbit $d_{3/2}$, the dimension is less than 10^6. However, the number of possible neutron configurations is beyond the capacity of shell-model calculations. As shown in Fig. 2, both level energies and spectroscopic factors decrease significantly when the number of valence neutrons increasing from ^{133}Sn to ^{137}Sn. With $l = 1$ transfer, the spectroscopic factors of states $3/2^-$ and $1/2^-$ in ^{137}Sn are 0.3 and 0.24, respectively, shrinking more than half. In ^{137}Sn, the spectroscopic factor of the ground state $7/2^-$ shrinks to 0.50 ($l = 3$), while the spectroscopic factor of state $13/2^+$ drops very slightly ($l = 6$). Without competition of cross-shell excitation by freezing orbits under $N = 82$, the state $13/2^+$ of ^{137}Sn has a good spectroscopic factor and keep single-particle properties very well.

V. LEVEL SPECTRA OF SN ISOTOPES

A. Odd-A

In ^{133}Sn, the low-lying levels of are selected as the single particle states in shell-model calculations, which have been observed in experiment [2]. The cross-shell excitations can be coupled with orbits $h_{11/2}$ and $d_{3/2}$ under the $N = 82$ shell in the present model space. As shown in Fig. 3, levels $1/2^+$ to $15/2^+$ have a main cross-shell configuration $\nu d_{3/2}^{-1} f_{7/2}^2$, which means that a neutron from orbit $d_{3/2}$ crosses the $N = 82$ shell and occupies the orbit orbit $f_{7/2}$. The high spin levels $17/2^+$ and $19/2^+$ have a main configuration $\nu h_{11/2}^{-1} f_{7/2} h_{9/2}$ that the cross-shell neutron comes from orbits $h_{11/2}$. The states $21/2^+$ and $23/2^+$ above 7 MeV have a main configuration $\nu h_{11/2}^{-1} f_{7/2} i_{13/2}$ coupled with the intruder orbit $i_{13/2}$. For negative parity levels, they have a main configuration $\nu h_{11/2}^{-1} f_{7/2}^2$ ($\geqslant 83\%$). The level $11/2^-$ at 3.6 MeV is lower than nearby states that form a spin-trap structure. This will block its decay from electromagnetic transitions, due to the limitation of selection rules.

The nucleus ^{135}Sn was first observed in the projectile fission of ^{238}U at a bombarding energy of 750 A MeV using a
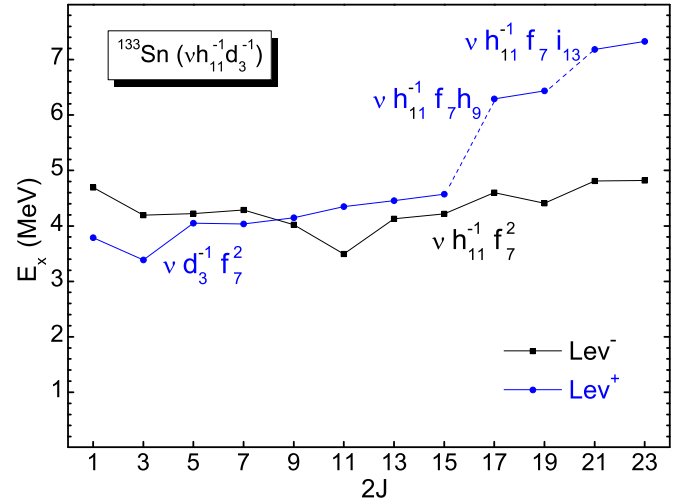

FIG. 3. Levels of cross-shell excitations with a main configuration (all $\geqslant 73\%$). The label ($\nu h_{11}^{-1} d_3^{-1}$) means allowing cross-shell excitation from both orbits $h_{11/2}$ and $d_{3/2}$. The exponent $-1(0)$ of orbit means allowing one (zero) neutron to cross the $N = 82$ shell.

Pb target [33]. Its half-life of ground state $7/2^-$ was measured at the Radioactive Isotope Factory [11]. However, there is no datum on its excited states yet. In ^{135}Sn, calculations are limited to show cross-shell exciting from both orbits $h_{11/2}$ and $d_{3/2}$. Instead of this situation, we provide results under three different cross-shell truncations (Fig. 4). The situation without core excitations ($\nu h_{11/2}^0 d_{3/2}^0$) is also listed as comparison. Here, the exponent "0" of orbit means no neutron excited from this orbit. The situation with core excitations only has little effects on negative parity levels. The ground state $7/2^-$ has a main configuration $\nu f_{7/2}^3$. The levels $5/2^-$, $9/2^-$, $11/2^-$, and $15/2^-$ are also belong to this configuration. The levels $17/2^-$,
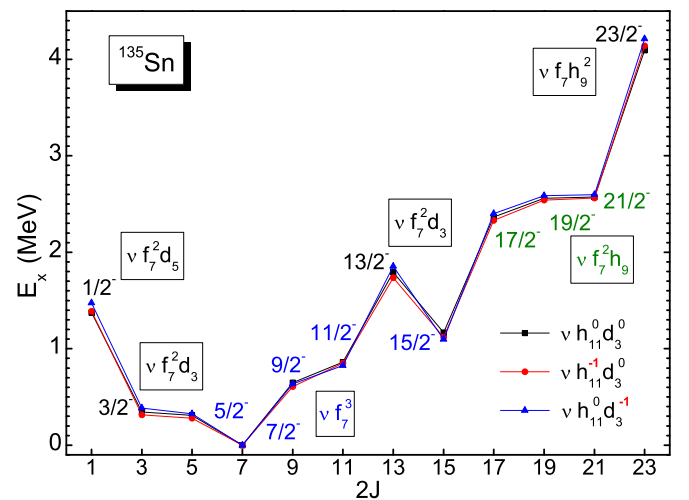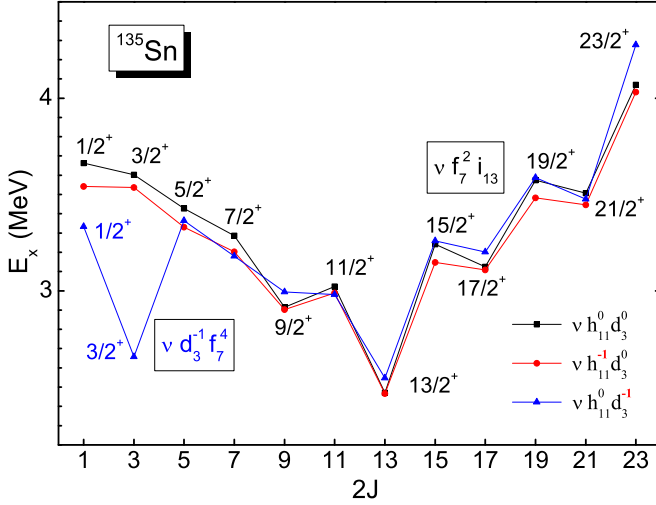

FIG. 4. The negative parity levels under three different truncations of cross-shell excitations (three labels in corner). The exponent $-1(0)$ of orbit means allowing one (zero) neutron to cross the $N = 82$ shell. Labels close to levels represent main configurations ($\geqslant 57\%$), except state $3/2^-$ ($\geqslant 37\%$) and $13/2^-$ ($\sim 41\%$).

FIG. 5. The positive parity levels under three different truncations of cross-shell excitations (three labels in corner). The exponent $-1(0)$ of orbit means allowing one (zero) neutron to cross the $N = 82$ shell. Labels close to levels represent main configurations (all $\geqslant 50\%$).

FIG. 7. The positive parity levels under three different truncations of cross-shell excitations (three labels in corner). The exponent $-1(0)$ of orbit means allowing one (zero) neutron to cross the $N = 82$ shell. Labels close to levels represent main configurations (all $\geqslant 68\%$). Corresponding data (Exp.) are from [32].

$19/2^-$, and $21/2^-$ about 2 MeV are members of configuration $\nu f_{7/2}^2 h_{9/2}$. The high spin level $23/2^-$ has a main configuration $\nu f_{7/2} h_{9/2}^2$.

For positive parity levels of ^{135}Sn (Fig. 5), levels from level $5/2^+$ to $23/2^+$ have a main configuration $\nu f_{7/2}^2 i_{13/2}$. In order to produce positive parity levels of ^{135}Sn, it is necessary to implicate the intruder $i_{13/2}$ orbital. The state $13/2^+$ at about 2.5 MeV is lower than levels nearby that forms a spin-trap structure, which would be a good isomer predicted firstly by this work. Levels $1/2^+$ and $3/2^+$ are core excitations of configuration $\nu d_{3/2}^{-1} f_{7/2}^4$ that a cross-shell neutron occupies the
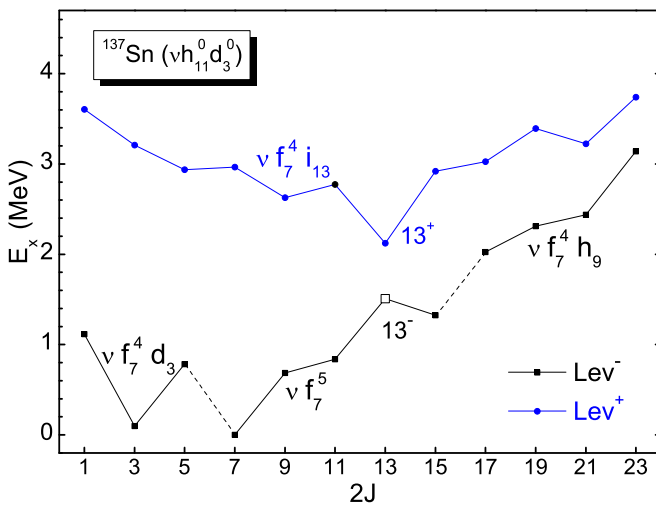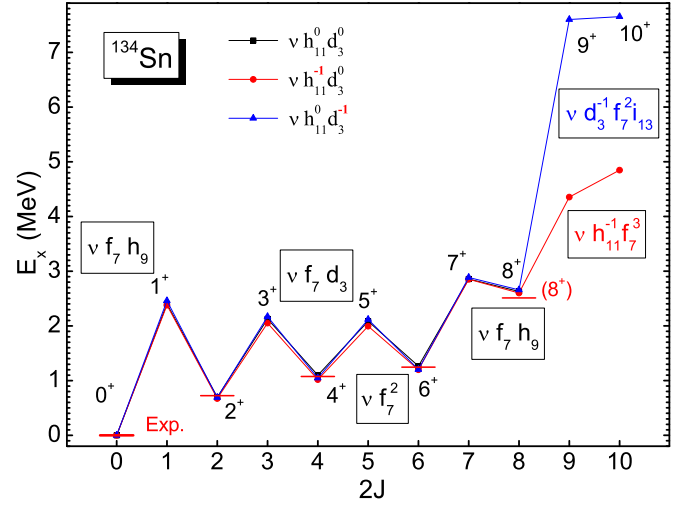

FIG. 6. The energy levels calculated without cross-shell excitations (label $\nu h_{11}^0 d_3^0$). Labels close to levels represent main configurations ($\geqslant 51\%$), except negative parity states of ($1/2^-$, $3/2^-$, $5/2^-$, $9/2^-$, $11/2^-$, and $13/2^-$ $\geqslant 26\%$) and positive parity states of ($5/2^+$, $9/2^+$, $13/2^+$, $15/2^+$, and $17/2^+$ $\geqslant 34\%$).

orbit $\nu f_{7/2}$ above the $N = 82$ shell. There is a large difference with or without core excitations in low-spin levels $1/2^+$ and $3/2^+$. Here, the level $3/2^+$ at 2.66 MeV is much lower than the state $3/2^+$ coupled by intruder orbit $i_{13/2}$.

In ^{137}Sn, the half-life of ground state was measured by decay curve of delayed neutrons [34]. we predict its ground state as $7/2^-$ with a main configuration $\nu f_{7/2}^5$ (52%). The levels $9/2^-$, $11/2^-$, and $15/2^-$ are also belong to this configuration (Fig. 6). The first excited state is predicted as level $3/2^-$ at 0.099 MeV, which has 42% of configuration $\nu f_{7/2}^4 d_{3/2}$, and 20% of configuration $\nu f_{7/2}^5$. Level $1/2^-$ has 40% of configuration $\nu f_{7/2}^4 d_{3/2}$, and 14% of configuration $\nu f_{7/2}^4 d_{5/2}$. Level $3/2^-$ has 42% of configuration $\nu f_{7/2}^4 d_{3/2}$, and 20% of configuration $\nu f_{7/2}^5$. Level $5/2^-$ has 26% of configuration $\nu f_{7/2}^4 d_{3/2}$, and 22% of configuration $\nu f_{7/2}^3 d_{5/2}^2$. Level $13/2^-$ has 48% of configuration $\nu f_{7/2}^4 d_{3/2}$. Level $15/2^-$ has a main configuration $\nu f_{7/2}^5$ (70%). Levels from $17/2^-$ to $23/2^-$ have a main configuration $\nu f_{7/2}^4 h_{9/2}$ ($\geqslant 57\%$). For positive parity levels, they have a main configuration $\nu f_{7/2}^4 i_{13/2}$ ($\geqslant 51\%$), except states of ($5/2^+$, $9/2^+$, $13/2^+$, $15/2^+$, and $17/2^+$ $\geqslant 34\%$). The level $13/2^+$ with 49% of configuration $\nu f_{7/2}^4 i_{13/2}$ is lower than nearby levels that form a spin-trap structure. In order to produce positive parity levels of ^{137}Sn, it is necessary to implicate the intruder $i_{13/2}$ orbital.

B. Even-A

The neutron spectra of ^{134}Sn was first investigated by Shalev and Rudstam [35]. As shown in Fig. 7, the levels 0^+, 2^+, 4^+, and 6^+ have a main configuration $\nu f_{7/2}^2$ ($\geqslant 68\%$), while the level 8^+ is coupled by configuration $\nu f_{7/2} h_{9/2}$ ($\geqslant 96\%$). The levels 1^+ and 7^+ have a main configuration $\nu f_{7/2} h_{9/2}$ ($\geqslant 95\%$), while levels
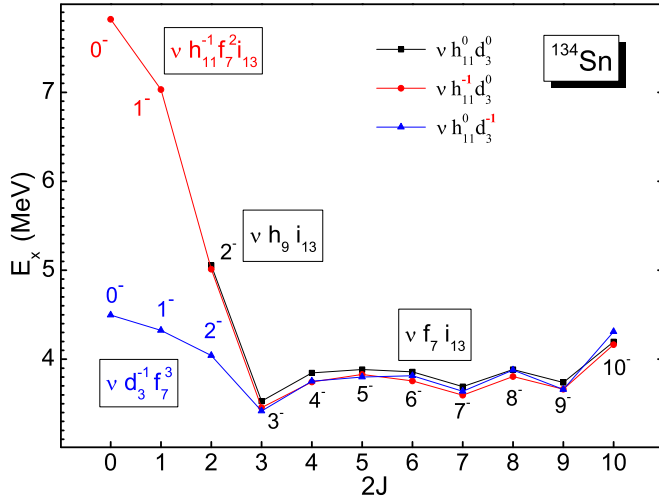
FIG. 8. The negative parity levels under three different truncations of cross-shell excitations (three labels in corner). The exponent $-1(0)$ of orbit means allowing one (zero) neutron to cross the $N = 82$ shell. Labels close to levels represent main configurations (all $\geqslant 75\%$).

FIG. 9. The positive parity levels under three different truncations of cross-shell excitations (three labels in corner). The exponent $-1(0)$ of orbit means allowing one (zero) neutron to cross the $N = 82$ shell. Labels close to levels represent main configurations ($\geqslant 55\%$), except 2^+ ($\geqslant 41\%$) and 5^+ ($\geqslant 49\%$). Corresponding data (Exp.) are from [32].

3^+ and 5^+ have a main configuration $\nu f_{7/2} d_{3/2}$ ($\geqslant 86\%$). The higher spin levels of 9^+ and 10^+ have a main configuration $\nu h_{11/2}^{-1} f_{7/2}^3$ ($\geqslant 84\%$) or $\nu d_{3/2}^{-1} f_{7/2}^2 i_{13/2}$ ($\geqslant 82\%$). They are cross-shell excitations with one neutron across the $N = 82$ shell. Here, the state 9^+ at 4.357 MeV excited from orbit $h_{11/2}$ is much lower than the level at 7.601 MeV excited from orbit $d_{3/2}$. For negative parity levels of ^{134}Sn, the intruder orbit $i_{13/2}$ is necessary to couple states from 3^- to 10^- (Fig. 8). In order to produce states with J^π from 3^- to 10^- (Fig. 8), it is necessary to implicate the intruder $i_{13/2}$ orbital.

These states have a main configuration $\nu f_{7/2} i_{13/2}$ ($\geqslant 75\%$). As cross-shell excitation, the level 2^- at 4.043 MeV is some lower than 2^- at 5.012 MeV coupled by intruder orbit $i_{13/2}$. Without core excitations (label $\nu h_{11/2}^0 d_{3/2}^0$), the model space can not produce states 0^- and 1^-. The states 0^- and 1^- above 4 MeV have a main cross-shell configuration $\nu d_{3/2}^{-1} f_{7/2}^3$ ($\geqslant 76\%$). The higher 0^- and 1^- states have a main configuration $\nu h_{11/2}^{-1} f_{7/2}^2 i_{13/2}$ ($\geqslant 87\%$). Note the level 3^- is always lower than nearby states among three different truncations. We predict this level 3^- as a good isomer, since the spin-trap structure can block its γ decay to lower levels.

The decay of neutron-rich ^{136}Sn was firstly studied at CERN/ISOLDE by using a resonance ionization laser ion source [36]. Lately, delayed γ-ray cascades have been observed from the decay of isomer (6^+) in semimagic nucleus ^{136}Sn [37]. As shown in Fig. 9, levels 0^+, 4^+, 6^+, and 8^+ have a main configuration $\nu f_{7/2}^4$ ($\geqslant 55\%$). Levels 2^+ and 5^+ have the biggest configuration $\nu f_{7/2}^4$ ($\geqslant 41\%$). Levels 1^+, 3^+, 7^+, and 9^+ have a main configuration $\nu f_{7/2}^3 d_{3/2}$ ($\geqslant 56\%$). Level 10^+ has a main configuration $\nu f_{7/2}^3 h_{9/2}$ ($\geqslant 79\%$). In order to produce states with J^π from 3^- to 10^- (Fig. 10), it is necessary to implicate the intruder $i_{13/2}$ orbital.

These states have a main configuration $\nu f_{7/2}^3 i_{13/2}$ ($\geqslant 57\%$), except states 4^- ($\geqslant 35\%$) and 5^- ($\geqslant 45\%$). The levels 0^-, 1^-,

and 2^- around 4 MeV have a big percentage of cross-shell configuration $\nu d_{3/2}^{-1} f_{7/2}^5$. The level 2^- at 3.690 MeV has 63% of configuration $\nu d_{3/2}^{-1} f_{7/2}^5$, which is much lower than the one coupled by orbits $f_{7/2}$ and $i_{13/2}$. Level 1^- at 3.960 MeV has 27% of cross-shell configuration $\nu d_{3/2}^{-1} f_{7/2}^5$, as well as 34% of configuration $\nu f_{7/2}^3 i_{13/2}$. The level 0^- at 4.174 MeV has 46% of cross-shell configuration $\nu d_{3/2}^{-1} f_{7/2}^5$, and 31% of another cross-shell configuration $\nu d_{3/2}^{-1} f_{7/2}^4 d_{3/2}$. The state 3^- forms a spin-trap structure whenever with or without core excitations.
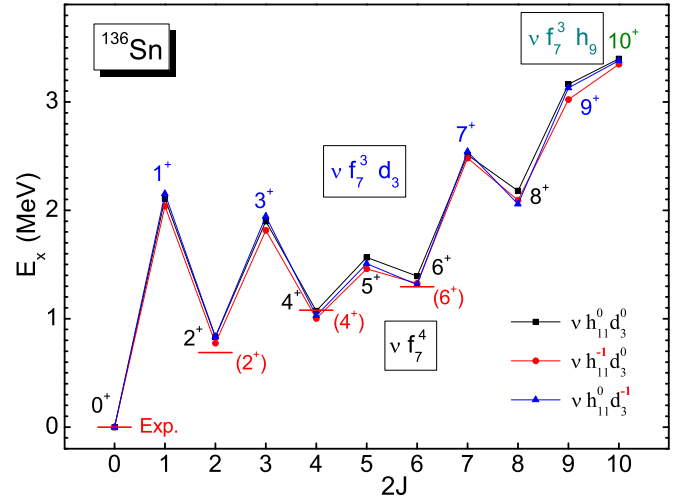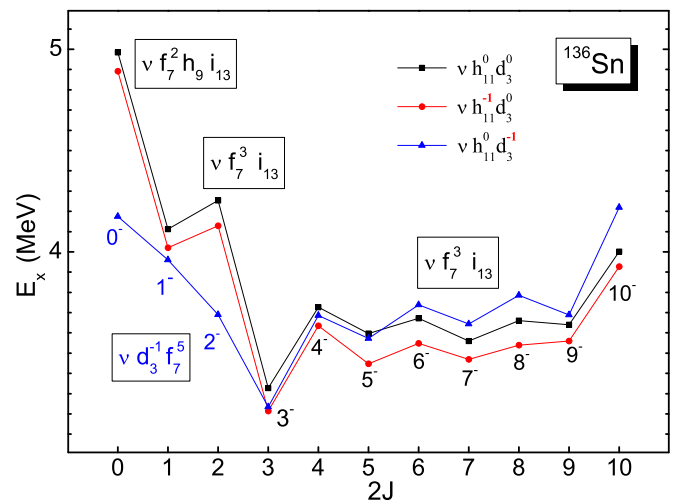

FIG. 10. The negative parity levels under three different truncations of cross-shell excitations (three labels in corner). The exponent $-1(0)$ of orbit means allowing one (zero) neutron to cross the $N = 82$ shell. Labels close to levels represent main configurations ($\geqslant 57\%$), except 0^- ($\geqslant 40\%$), 1^- ($\geqslant 27\%$), 4^- ($\geqslant 35\%$), and 5^- ($\geqslant 45\%$).

This state 3^- of ^{136}Sn is predicted as a good isomer, due to the γ decay blocked by the spin-trap structure.

VI. CONCLUSIONS

In this work, we investigate spectroscopic factors and level spectra in neutron-rich Sn isotopes with the model space including both core excitations and intruder orbit $i_{13/2}$. Here are the main conclusions:

(1) In ^{131}Sn, the second group of single particle states is well investigated by spectroscopic factors and configurations. The state $13/2^+$ is predicted at 4.8 MeV with a small value of spectroscopic factor relatively (about 0.20). The configurational structure shows that the competition driven by double cross-shell excitations weakens the single particle properties of this high-lying state $13/2^+$.

(2) In ^{133}Sn, the low-lying states and cross-shell excitations are studied from level $1/2^-$ ($1/2^+$) to $23/2^-$ ($23/2^+$). With a spin-trap structure, the level $11/2^-$ at 3.6 MeV is predicted as a good isomer coupled by cross-shell configuration $\nu h_{11/2}^{-1} f_{7/2}^2$.

(3) In order to produce positive-parity states of ^{135}Sn, it is necessary to implicate the intruder $i_{13/2}$ orbital. The state $3/2^+$ is predicted at 2.66 MeV with a main cross-shell configuration $\nu d_{3/2}^{-1} f_{7/2}^4$. With a spin-trap structure, the state $13/2^+$ at about 2.5 MeV is predicted as a good isomer coupled by intruder orbit $i_{13/2}$.

(4) In order to produce negative-parity states of ^{134,136}Sn, it is necessary to implicate the intruder $i_{13/2}$ orbital. The level 3^- is predicted as a good isomer in ^{134}Sn (^{136}Sn), due to the γ decay blocked by the spin-trap structures.

(5) In ^{137}Sn, the ground state is predicted as level $7/2^-$ with a main configuration $\nu f_{7/2}^5$ (52%). The level $13/2^+$ is predicted at about 2.1 MeV with 49% of configuration $\nu f_{7/2}^4 i_{13/2}$, which is lower than nearby levels that forms a spin-trap structure. Without competition of cross-shell excitation by freezing orbits under $N = 82$, this state $13/2^+$ of ^{137}Sn has a good single-particle property indicated by spectroscopic factor.

The results of this study can provide insight into the behavior of nucleons at the limits of stability and aid in the understanding of the properties of neutron-rich nuclei. This research emphasizes the importance of the intruder orbit $i_{13/2}$ to explain level spectra of neutron-rich Sn isotopes. These predictions should provide useful guidance for further experiments in these nuclei regions.

[1] M. G. Mayer and J. H. D. Jensen, *Theory of Nuclear Shell Structure* (Wiley, New York, 1955).

[2] K. L. Jones, A. S. Adekola, D. W. Bardayan, J. C. Blackmon, K. Y. Chae, K. A. Chipps, J. A. Cizewski, L. Erikson, C. Harlin, R. Hatarik, R. Kapler *et al.*, Nature (London) **465**, 454 (2010).

[3] B. A. Brown, N. J. Stone, J. R. Stone, I. S. Towner, and M. Hjorth-Jensen, Phys. Rev. C **71**, 044317 (2005).

[4] K. L. Jones, F. M. Nunes, A. S. Adekola, D. W. Bardayan, J. C. Blackmon, K. Y. Chae, K. A. Chipps, J. A. Cizewski, L. Erikson, C. Harlin *et al.*, Phys. Rev. C **84**, 034601 (2011).

[5] M. Mumpower, R. Surman, G. McLaughlin, and A. Aprahamian, Prog. Part. Nucl. Phys. **86**, 86 (2016).

[6] O. Sorlin and M. G. Porquet, Prog. Part. Nucl. Phys. **61**, 602 (2008).

[7] C. Gorges, L. V. Rodriguez, D. L. Balabanski, M. L. Bissell, K. Blaum, B. Cheal, R. F. Garcia Ruiz, G. Georgiev, W. Gins, H. Heylen, A. Kanellakopoulos, S. Kaufmann, M. Kowalska, V. Lagaki, S. Lechner, B. Maass, S. Malbrunot-Ettenauer, W. Nazarewicz, R. Neugart, G. Neyens, W. Nortershauser, P. G. Reinhard, S. Sailer, R. Sanchez, S. Schmidt, L. Wehner, C. Wraith, L. Xie, Z. Y. Xu, X. F. Yang, and D. T. Yordanov, Phys. Rev. Lett. **122**, 192502 (2019).

[8] H. K. Wang, Z. H. Li, Y. B. Wang, and B. Jiang, Phys. Lett. B **833**, 137337 (2022).

[9] B. A. Brown, W. A. Richter, and R. Lindsay, Phys. Lett. B **483**, 49 (2000).

[10] J. J. Cowan, F.-K. Thielemann, and J. W. Truran, Phys. Rep. **208**, 267 (1991).

[11] G. Lorusso, S. Nishimura, Z. Y. Xu, A. Jungclaus, Y. Shimizu, G. Simpson, P.-A. Soderstrom, H. Watanabe, F. Browne, and P. Doomenbal, Phys. Rev. Lett. **114**, 192501 (2015).

[12] J. M. Allmond, A. E. Stuchbery, J. R. Beene, A. Galindo-Uribarri, J. F. Liang, E. Padilla-Rodal, D. C. Radford, R. L. Varner, A. Ayres, J. C. Batchelder, A. Bey, C. R. Bingham, M. E. Howard, K. L. Jones, B. Manning, P. E. Mueller, C. D. Nesaraja, S. D. Pain, W. A. Peters, A. Ratkiewicz, K. T. Schmitt, D. Shapira, M. S. Smith, N. J. Stone, D. W. Stracener, and C. H. Yu, Phys. Rev. Lett. **112**, 172701 (2014).

[13] B. A. Brown and B. H. Widenthal, Annu. Rev. Nucl. Part. Sci. **38**, 29 (1988).

[14] M.-G. Porquet, T. Venkova, R. Lucas, A. Astier, A. Bauchet, I. Deloncle, A. Prevost, F. Azaiez, G. Barreau, A. Bogachev *et al.*, Eur. Phys. J. A **24**, 39 (2005).

[15] H. K. Wang, Y. Sun, H. Jin, K. Kaneko, and S. Tazaki, Phys. Rev. C **88**, 054310 (2013).

[16] H. K. Wang, S. K. Ghorui, K. Kaneko, Y. Sun, and Z. H. Li, Phys. Rev. C **96**, 054313 (2017).

[17] P. Hoff *et al.*, Phys. Rev. Lett. **77**, 1020 (1996).

[18] W. Urban, W. Kurcewicz, A. Nowak, T. Rzaca-Urban *et al.*, Eur. Phys. J. A **5**, 239 (1999).

[19] J. Escher and B. K. Jennings, Phys. Rev. C **66**, 034313 (2002).

[20] H. K. Wang, K. Kaneko, and Y. Sun, Phys. Rev. C **89**, 064311 (2014).

[21] H. K. Wang, K. Kaneko, Y. Sun, Y. Q. He, S. F. Li, and J. Li, Phys. Rev. C **95**, 011304(R) (2017).

[22] H. K. Wang, S. K. Ghorui, Z. Q. Chen, and Z. H. Li, Phys. Rev. C **102**, 054316 (2020).

[23] H. K. Wang, Z. Q. Chen, H. Jin, Z. H. Li, G. S. Li, Y. M. Feng, and Q. Wang, Phys. Rev. C **104**, 014301 (2021).

[24] R. L. Kozub, G. Arbanas, A. S. Adekola, D. W. Bardayan, J. C. Blackmon, K. Y. Chae, K. A. Chipps, J. A. Cizewski, L. Erikson, R. Hatarik *et al.*, Phys. Rev. Lett. **109**, 172501 (2012).

[25] H. K. Wang, G. X. Li, B. Jiang, and Y. B. Qian, Phys. Rev. C **106**, 054316 (2022).

[26] B. A. Brown and W. D. M. Rae, Nucl. Data Sheets **120**, 115 (2014).

[27] N. Shimizu, Nuclear shell-model code for massive parallel computation, KSHELL, arXiv:1310.5431 (2013).

[28] A. P. Zuker, Phys. Rev. Lett. **90**, 042502 (2003).

[29] Y. Z. Ma, L. Coraggio, L. D. Angelis, T. Fukui, A. Gargano, N. Itaco, and F. R. Xu, Phys. Rev. C **100**, 034324 (2019).

[30] B. A. Brown, *Lecture Notes in Nuclear Structure Physics* (Michigan State University, E. Lansing, MI, 2005).

[31] A. Bohr and B. R. Mottelson, *Nuclear Structure* (World Scientific, Singapore, 2005), first published in 1998.

[32] National Nuclear Data Center, Data extracted using the NNDC Online Data Service from the ENSDF database, with nucleus (cutoff dates) of ^{134}Sn (31 July 2004) and ^{136}Sn (1 April 2018), http://www.nndc.bnl.gov.

[33] M. B. S. Czajkowski, P. Armbruster, H. Geissel, P. Dessagne, C. Donzaud, H.-R. Faust, E. Hanelt, A. Heinz, M. Hesse *et al.*, Phys. Lett. B **331**, 19 (1994).

[34] O. Arndt, K. L. Kratz, W. B. Walters, K. Farouqi, U. Koster, V. Fedosseev, S. Hennrich, C. J. Jost, A. Wohr, A. A. Hecht, B. Pfeiffer, J. Shergur, and N. Hoteling, Phys. Rev. C **84**, 061307(R) (2011).

[35] S. Shalev and G. Rudstam, Nucl. Phys. A **230**, 153 (1974).

[36] J. Shergur, M. Hanawald, D. Seweryniak, H. Fynbo, U. Koester, A. Woehr, D. Fedorov, V. Fedoseyev, V. Mishin, P. Hoff *et al.*, Nucl. Phys. A **682**, 493 (2001).

[37] G. Lorusso, Nishimura, Z. Y. Xu, A. Jungclaus, Y. Shimizu, G. S. Simpson, P.-A. Söderström, H. Watanabe, F. Browne, P. Doomenbal *et al.*, Phys. Rev. Lett. **113**, 132502 (2014).